An Amperometric Solid-State Gas Sensor Using a $LaGaO_3$-Based Perovskite Oxide Electrolyte for Detecting Hydrocarbon in Exhaust Gas. A Bimetallic Anode for Improving Sensitivity at Low Temperature

Atanu Dutta,*,† Tatsumi Ishihara,† and Hiroyasu Nishiguchi‡

Departments of Applied Chemistry, Faculties of Engineering, Kyushu University, Hakozaki 6-10-1, Higashi-Ku, Fukuoka 812-8581, and Oita University, Dannoharu 700, Oita 870-1192, Japan

Received May 14, 2004. Revised Manuscript Received September 14, 2004

For the first time, an amperometric electrochemical sensor based on $LaGaO_3$ was demonstrated as highly sensitive to detect hydrocarbon (C_3H_6) at low temperature (423−773 K). At this temperature range, it is very important to estimate hydrocarbon pollution of automobile exhaust gas (the cold start condition). In the present study, using $La_{0.5}Sr_{0.5}MnO_3$ as the oxygen reduction electrode, various hydrocarbon (C_3H_6) oxidation electrodes of Pt-based alloy systems were investigated. Addition of Co and subsequently cermet LDC $[(CeO_2)_{0.8}(LaO_{1.5})_{0.2}]$ produced very high sensor response and improved the performance of the sensor with respect to that using only Pt paste as the electrode. The sensors were hardly influenced by the oxygen concentration variation (0.5−5%). At the best operating temperature (623 K) the C_3H_6 sensitivity was above 800 μA/decade, and the lowest temperature of detection was 423 K. The sensors were fast, highly selective in the presence of coexisting gases, e.g., NO, NO_2, CO, and H_2, in the exhaust, and stable too. Sensors studied in the potentiometric mode and with impedance analysis of the hydrocarbon oxidation electrodes revealed the importance of the electrolyte/electrode interface and the related sensing mechanism.

Introduction

Investigation of selective and reliable sensors for the detection of automobile exhaust gas pollution is an important area of sensor research these days. Use of a three-way catalyst assembly ensures the removal of 90% pollution in exhaust gas from internal combustion engines. But this converter along with the λ-sensor (to maintain the air-to-fuel ratio at 14.7) cannot work unless the engine is sufficiently heated above 873 K. Incidentally, in the first 1−2 min at cold start of the engine, emission of unburnt hydrocarbon is significant and may deteriorate the environment with photochemical smog. The excessive hydrocarbon emission means extra fuel loss, and this causes degradation of the three-way catalyst. Therefore, in addition to oxygen sensors, usage of a sensor is required for detecting this hydrocarbon leakage, and appropriate measures can be taken to stop unnecessary emission.

To meet this demand, a hydrocarbon sensor operating at low temperature (below 673 K) needs to be developed. Normally, semiconductor sensors[1−3] are demonstrated for hydrocarbon sensing in such a low-temperature range. However, due to high surface reactivity, these sensors often lack selectivity for a particular gas. The selectivity of the sensor is an important factor for exhaust gas operating conditions. The electrochemical sensors based on a solid electrolyte normally operate at higher temperature (>773 K) and have better selectivity. But the magnitude of the output signal is small at temperatures below 873 K due to low ionic conductivity and slow electrode reactions. Recently, few theoretical and experimental investigations have been done on the cold start condition of the engine.[4−8] Wingbrant et al.[4] have reported the MISiCFET sensor using silicon carbide at 773 K for cold start conditions of the engine. Zosel et al.[8] studied a zirconia-based potentiometric hydrocarbon sensor with various composite and perovskite oxides as the electrode above 973 K. It is well-known that $LaGaO_3$ electrolyte has much higher ionic

---

[*] To whom correspondence should be addressed. E-mail: atanu@cstf.kyushu-u.ac.jp.

[†] Kyushu University.

[‡] Oita University.

(1) Rosental, A.; Tarre, A.; Gerst, A.; Sundqvist, J.; Hårsta, A.; Aidla, A.; Aarik, J.; Sammelselg, V.; Uustare, T. *Sens. Actuators, B: Chem.* **2003**, *93*, 552.

(2) Lee, Y.-S.; Kwon, O.-S.; Lee, S.-M.; Song, K.-D.; Shim, C.-H.; Rue, G.-H.; Lee, D.-D. *Sens. Actuators, B: Chem.* **2003**, *93*, 556.

(3) Chatterjee, K.; Chatterje, S.; Banerjee, A.; Raut, M.; Pal, N. C.; Sen A.; Maiti, H. S. *Mater. Chem. Phys.* **2003**, *81*, 33.

(4) Wingbrant, H.; Svenningstop, H.; Salomonsson, P.; Tengström, P.; Lundström, I.; Spetz, A. L. *Sens. Actuators, B: Chem.* **2003**, *93*, 295.

(5) Liu, X.; Lampert, J. K.; Arendarskiia, D. A.; Farrauto, R. J. *Appl. Catal., B: Environ.* **2001**, *35*, 125.

(6) Chakravarthy, V. K.; Conklin, J. C.; Daw, C. S.; D'Azevedo, E. F. *Appl. Catal., A: Gen.* **2003**, *241*, 289.

(7) Botsaris, P. N.; Bechrakis, D.; Sparis, P. D. *Appl. Catal., A: Gen.* **2003**, *243*, 285.

(8) Zosel, J.; Ahlborn, K.; Muller, R.; Westphal, D.; Vashook, V.; Guth, U. *Solid State Ionics* **2004**, *169*, 115.

10.1021/cm049242e CCC: $27.50

conductivity compared with other electrolytes[9,10] such as YSZ and doped CeO_2. For solid oxide fuel cell applications, this is one of the most important features of the operation at intermediate temperature (773−1073 K). For sensor applications in the low-temperature range, though there could be a contribution from electronic hole conductivity, the ionic conductivity is still large enough to generate sensor output current as a result of electrochemical reactions. In addition to this, it is also important that the chemical reactivity of both the active and inactive electrodes be very high at the low-temperature operation of the sensor device. Hence, the investigation of suitable electrode materials is an interesting aspect of this sensor research.

In our previous work,[11] it was demonstrated that a $La_{0.8}Sr_{0.2}Ga_{0.8}Mg_{0.1}Ni_{0.1}O_3$ electrolyte based sensor with a Pt anode gave the best performance for C_3H_6 in the temperature range 523−673 K when $La_{0.5}Sr_{0.5}MnO_3$ was used as the cathode. Commercial Pt paste containing various additives and organic binders generally poses problems for long-term usage, and in most cases, the overall performance of the device deteriorates with time. So, in the present work, we searched for an alternate active electrode material, intending further enhancement of the sensing performance for C_3H_6. Extracting Pt from tetraammineplatinum(II) nitrate, we investigated the addition of various metals and/or metal oxides to Pt to improve the hydrocarbon sensing characteristics at low temperature (423−673 K). The results demonstrated (Pt + 10% Co) (90%) + LDC (10%) as the optimal active electrode combination. The sensing mechanism was proposed on the basis of the mixed potential theory. The developed sensors were found to be stable, highly sensitive, and selective for C_3H_6.

Experimental Section

Preparation of $La_{0.8}Sr_{0.2}Ga_{0.8}Mg_{0.1}Ni_{0.1}O_3$ (denoted as LSGMN) solid electrolyte and $La_{0.5}Sr_{0.5}MnO_3$ (denoted as LSM 55) was described in our previous paper.[11] For the preparation of a Pt-based alloy anode, tetraammineplatinum(II) nitrate (Aldrich Chemical Co.) as the Pt source was mixed with metal nitrate (Wako) in the appropriate amount in deionized water. The resultant mixture was constantly stirred on a hot plate until dry. Finally, the accumulated powder was calcined at 673 K for 6 h in air. A slurry of this powder was painted onto one face of an LSGMN disk (0.4 mm thickness) as the active electrode. On the other side, LSM 55 was painted as the inactive electrode. A schematic diagram of the sensor fabrication is shown in Figure 1. XRD measurement of LSGMN and the active electrode material was carried out with a Ragaku Rint 2000, Cu Kα line.

In the measurement assembly, the sensor device was placed in the single environment of either reference gas (1% O_2 in N_2) or sample gas C_3H_6 in parts per million mixed with 1% O_2 in N_2. In the amperometric mode, keeping the active electrode at +1 V bias, the current was registered with respect to time every 10 s. A Kenwood model PA18-3A was used as the dc power source. The voltage was measured with a digital multimeter (Advantest, model R645A) and/or digital electrometer (Advantest, model R8240).

The complex impedance spectral measurements were performed using a Solartron impedance analyzer (type 1260) in the frequency range from 10^6 to 0.001 Hz. In the open circuit mode, the amplitude of the sinusoidal voltage signal was 5 mV. Measurements were done at different temperatures and both in the reference gas and in the sample gas. Platinum was used as the reference electrode.

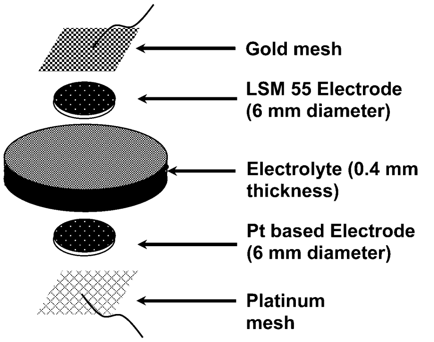

Figure 1. Schematic diagram of the fabricated sensor.

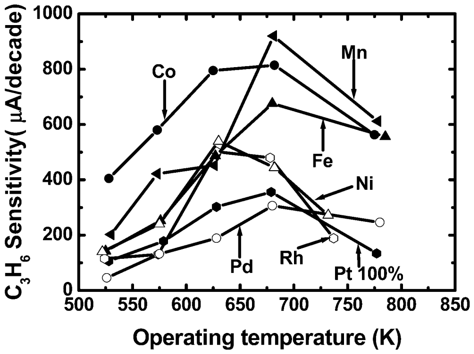

Figure 2. Temperature dependence of sensitivity on the LSGMN electrolyte based sensors with LSM 55 inactive electrode and Pt + 10 wt % metal (Co, Mn, Fe, Ni, Rh, and Pd) active electrodes.

Results and Discussion

Improvement of the Catalytic Activity of the Active Electrode. In our previous study, keeping Pt paste as the active electrode, the effects of the inactive electrode were investigated and the inactive electrode composition was optimized as $La_{0.5}Sr_{0.5}MnO_3$ (LSM 55). In the present work, keeping LSM 55 as the inactive electrode, the effects of an additive to Pt were studied for increasing the activity for oxidation of the hydrocarbon. It is reported in the literature that the addition of noble metals to the anode composition effectively increases the cell power density and improves the performance of SOFC with hydrocarbon fuel.[12,13] The metal alloy electrode enhances the catalytic activity for hydrocarbon combustion. Figure 2 shows the effects of a 10 wt % additive to Pt on the sensitivity to C_3H_6. It was observed that the addition of a small amount of metal to Pt was effective for enhancing the sensitivity to C_3H_6. Incidentally, the catalytic oxidation reaction of C_3H_6 may have increased with additives in comparison with that of 100% Pt as the oxidation electrode. Addition of a small amount of metal also effectively increased the base current of the sensors, which means the current in the reference gas flow. Among the

---

(9) Ishihara, T.; Matsuda, H.; Takita, Y. *J. Am. Ceram. Soc.* **1994**, *116*, 3801.

(10) Zheng, F.; Bordia, R. K.; Pederson, L. R. *Mater. Res. Bull.* **2004**, *39*, 141.

(11) Dutta, A.; Ishihara, T.; Nishiguhci, H.; Takita, Y. *J. Electrochem. Soc.* **2004**, *151*, H122.

(12) Hibino, T.; Hashimoto, A.; Asano, K.; Yano, M.; Suzuki, M.; Sano, M. *Electrochem. Solid State Lett.* **2002**, *5*, A242.

(13) McIntosh, S.; Vohs, J. M.; Gorte, R. J. *Electrochem. Solid State Lett.* **2003**, *6*, A240.

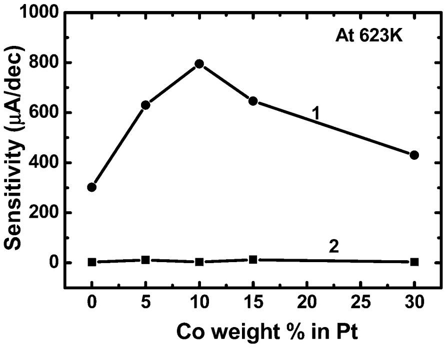

Figure 3. Sensitivity as a function of Co added to Pt as the active electrode at 623 K: (1) C_3H_6 sensitivity; (2) oxygen sensitivity (keeping the C_3H_6 concentration fixed to 1000 ppm; the O_2 concentration was varied from 0.5% to 5%).

investigated additives, it was found that addition of Mn or Co is effective for increasing the sensitivity. It is well-known that the oxide of these two metals is highly active in oxidation reaction. Improvement of the sensitivity to C_3H_6 could be explained by increased activity of the Pt–metal electrode for C_3H_6 oxidation. In the case of Mn addition, the sensitivity increase at high temperature (around 700 K) was significant. In contrast, the sensitivity at low temperature (around 600 K) was greatly improved by adding Co. Although the highest sensitivity was obtained with Mn addition, a further detailed study of the sensor characteristics was performed with the Pt–Co system. No significant dependency on oxygen was observed for the sensor using a Pt–Co electrode in the P_{O_2} range from 0.5% to 5%.

Figure 3 shows the sensitivity to C_3H_6 and O_2 at 623 K for the sensors with an active electrode as a function of the Co amount added to Pt. The sensitivity to C_3H_6 was strongly dependent on the amount of Co, and it is seen that the highest sensitivity was achieved at 10 wt % Co. On the other hand, the sensitivity to O_2 was negligibly small, and it is hardly dependent on the Co amount. In our study, the sensor using pure Co as the electrode exhibited very low current output and poor sensitivity to C_3H_6 (21 μA/decade at 623 K). Therefore, an excess amount of Co only decreases the sensitivity to C_3H_6. As a result, the optimum amount of Co addition seems to be around 10 wt % Co. For this sensor, the sensitivity to C_3H_6 was as high as 800 μA/decade, which is almost 2.5 times higher than that of pure Pt as the active electrode.

Since the electrochemical reactions occur at the triple-phase boundary among the solid electrolyte, electrode, and gas phase, it is expected that the addition of an oxide ion conductor could improve the performance of the electrode. Hence, 10 wt % concentrations of four different oxide ion conductors, e.g., LDC [$(CeO_2)_{0.8}(LaO_{1.5})_{0.2}$], SDC [$Ce_{0.8}Sm_{0.2}O_2$], PrDC [$Ce_{0.8}Pr_{0.2}O_2$], and LSGMN [$La_{0.8}Sr_{0.2}Ga_{0.8}Mg_{0.1}Ni_{0.1}O_3$], were added to Pt + 10% Co as the active electrode of the sensor. Figure 4 shows the temperature dependence of the sensitivity to C_3H_6 of the sensor using an oxide-mixed Pt–Co system as the active electrode. At the same precalcination temperature (i.e., 1123 K) as for the inactive electrode (LSM 55), the sensor showed deterioration of the sensitivity by mixing an oxide ion conductor with the Pt base electrode. It was also observed that the base current decreased appreciably by mixing with oxide. The high contact resistance between the electrode and electrolyte could be the reason for the low response. In this study, the effect of the precalcination temperature on the active electrode was further studied by using an LDC-mixed Pt–Co electrode. As expected, the sensor performance improved with increasing precalcination temperature, and the highest sensitivity was achieved when the precalcination was performed at 1573 K for 1 h. Therefore, in Figure 4, the sensitivity to C_3H_6 is shown for the sensors which are precalcined at 1573 K for 1 h for the active electrode followed by precalcination of the inactive electrode at 1123 K. Although the sensitivity did not significantly change by mixing the different oxide ion conductors for the active electrode, there was a marginal increase of the sensitivity with respect to the Pt + 10% Co electrode at all the temperatures. Among the examined oxide ion conductors, mixing LDC with Pt–Co gave the highest sensitivity at 623 K. Therefore, in this study, Pt–Co mixed with LDC was further studied in detail as the active electrode.

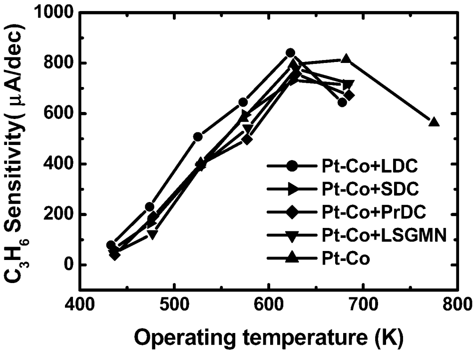

Figure 4. Effects of an oxide ion conductor mixed with Pt–Co as the oxidation electrode on the sensitivity to C_3H_6 [LDC, [$(CeO_2)_{0.8}(LaO_{1.5})_{0.2}$]; SDC, [$Ce_{0.8}Sm_{0.2}O_2$]; PrDC, [$Ce_{0.8}Pr_{0.2}O_2$]; LSGMN, [$La_{0.8}Sr_{0.2}Ga_{0.8}Mg_{0.1}Ni_{0.1}O_3$]].

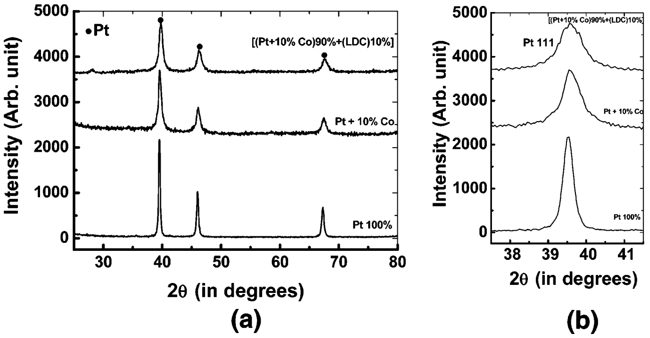

Figure 5. (a) X-ray powder diffraction patterns of pure Pt (100%), Pt + 10% Co, and (Pt + 10% Co) (90%) + LDC (10%). (b) Enlarged peak position corresponding to the (111) plane.

To check the chemical state of Co added to Pt after precalcination at 1573 K, XRD measurement was performed on the Pt + 10% Co powder sample. XRD analyses of the powder sample of 100% Pt and the Pt–Co–LDC system were also done. The results are shown in Figure 5a. It can be seen that all the diffraction peaks are assigned to those from Pt. However, no diffraction peak from Co or a Co-containing compound was observed. Figure 5b shows the enlarged XRD peak of the (111) plane. There is a shift of the diffraction angle of the Pt–Co system with respect to that of pure Pt. In addition, no shift of the peaks was observed by mixing

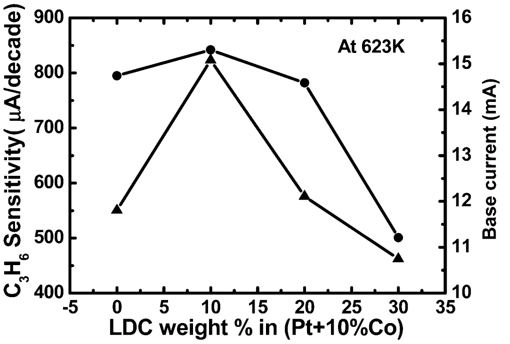

Figure 6. Effect of LDC amount added (wt %) to Pt + 10% Co on the hydrocarbon sensitivity and base current of the sensor operating at 623 K.

Table 1. Comparison of the Base Current Using Different Active Electrodes

temp (K)	base current (mA)		
	100% Pt	Pt + 10% Co	(Pt + 10% Co) (90%) + LDC (10%)
523	1.339	3.952	5.177
573	2.354	6.665	9.412
623	4.210	11.805	15.080
673	6.260	17.700	>20.000

LDC with Pt−Co. On the basis of the cubic structure of the Pt unit cell, the lattice parameter was estimated. The obtained *a* value for Pt and Pt−Co is 393.93 and 393.30 pm, respectively. It is clear that the lattice parameter of Pt shrank with addition of Co. Considering the atomic radius of Co (152 pm) to be smaller than that of Pt (177 pm), shrinkage of the lattice parameter is reasonably explained by formation of a solid solution of Co in Pt. The state of Co was also confirmed by XPS analysis, and the chemical state of Co in the Pt−Co electrode is metallic. LDC might be considered as dispersed in the Pt−Co system without going into a solid solution.

It was stated before that the increase in sensitivity was not so large by mixing LDC with the Pt−Co system, but it was found that the base current of the sensor increased largely by mixing an oxide ion conductor for the active electrode. Table 1 shows the base current of the sensors for the three active electrodes at different operating temperatures. The current increased in the following order: Pt < Pt−10 wt % Co ≪ Pt−10 wt % Co + 10 wt % LDC. The base current is another important factor for the amperometric sensor when the sensor is put into practical application. For a high current output value, the signal treatment becomes much easier and the S/N ratio is also much improved. Therefore, from the viewpoint of the actuator circuit, introduction of an oxide ion conductor for the active electrode is promising. It is also interesting to note that the base current at a low temperature such as 423 K was also sufficiently high and the sensitivity was 50 μA/decade. This suggests that the sensor could be operated at such a low temperature.

An LDC-mixed active electrode was further investigated to optimize the amount of LDC. Figure 6 shows the sensitivity to C_3H_6 as a function of the LDC amount at 623 K. The sensitivity slightly increased with increasing amount of LDC, and the highest sensitivity was obtained on the sensor using a 10 wt % LDC-mixed Pt−Co anode. As shown in Figure 6, the base current progressively decreased with increasing LDC amount beyond 10% in the electrode composition. This can be attributed to the increase in the electrode resistance, and hence, the sensor response decreased as the LDC amount increased. Thus, the optimal composition for the active anode was achieved at (90% Pt + 10% Co) (90%) + LDC (10%) in weight ratio.

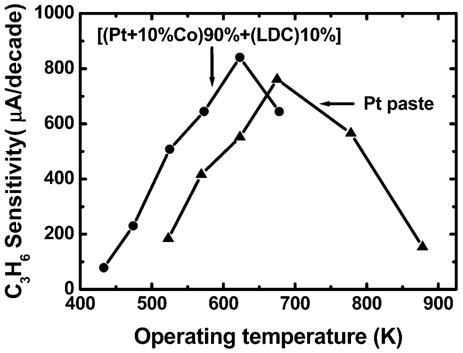

Figure 7. Comparison of the temperature dependence of C_3H_6 sensitivity for the LSGMN-based sensor with Pt−Co−LDC cermet and Pt paste as the active electrode.

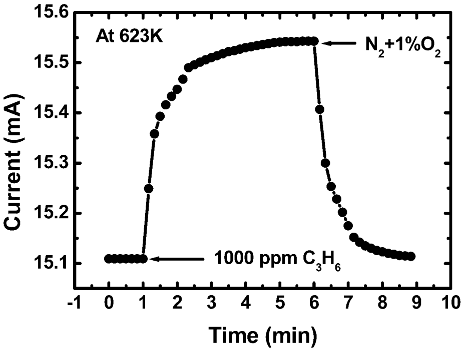

Figure 8. Current response characteristic of the LSM 55/LSGMN/Pt−Co−LDC sensor with respect to time in the presence of 1000 ppm C_3H_6 at 623 K.

Sensing Properties of a Hydrocarbon Sensor using a Pt−Co−LDC Cermet Electrode. Figure 7 shows the temperature dependence of the sensitivity to C_3H_6 of the sensor using the optimal active electrode, (90% Pt + 10% Co) (90%) + LDC (10%), in comparison with that of the previous sensor using Pt paste.[11] It is seen that the sensitivity is much improved by using the cermet electrode; in particular, the increase in the low-temperature range is significant. Since the oxidation activity of the Pt alloy electrode greatly improved, the temperature at which the highest sensitivity was achieved was shifted to lower temperature by 50 K, and hence, the optimum operation temperature of the present sensor was found to be around 623 K.

The typical current response of the sensor at 623 K is shown in Figure 8. The current increased steadily with the introduction of 1000 ppm C_3H_6 in the sensing gas. After exposure to a base gas (N_2−1%O_2) atmosphere, the current recovered to the original level quickly. The response and the recovery times for 90% of the saturation current value are 80 and 110 s, respectively. Considering the period for exchanging the gas in the measurement chamber, which is estimated to be 30 s, this sensor can be considered as reasonably fast.

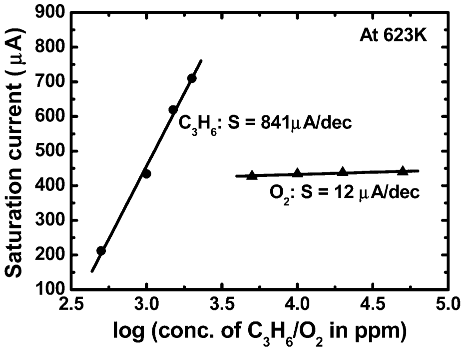

Figure 9. Saturation current of the sensor output as a function of C_3H_6 concentration (with 1% oxygen) and oxygen concentration (with 1000 ppm C_3H_6).

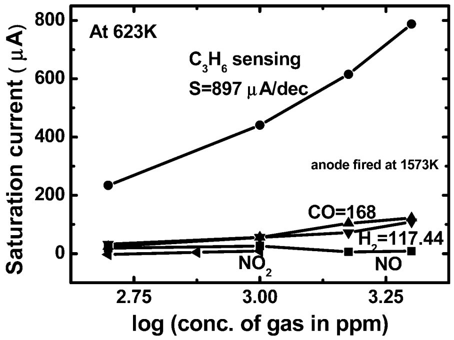

Figure 10. Saturation current of the sensor output as a function of the concentration of various gases at 623 K.

Figure 9 shows the saturation current for various C_3H_6 concentrations. It is obvious that the saturation current monotonically depends on the logarithm of the C_3H_6 concentration. Therefore, the concentration of the hydrocarbon can easily be estimated from the current of the sensor. The current output of the sensor to 1000 ppm C_3H_6 is also shown in Figure 9 as a function of the O_2 concentration. For this sensor, a different activity of the electrode catalyst for the oxidation of C_3H_6 was used, so the sensor response might also be affected by P_{O_2} in a deficient amount of oxygen. However, when the amount of oxygen coexists sufficiently, it is obvious that the current to 1000 ppm C_3H_6 is hardly affected by the oxygen concentration. This property is ideal for monitoring of hydrocarbon in exhaust gas. This is because the oxygen concentration in exhaust gas is varied frequently in accordance with the combustion mode of engines. Thus, using the present sensor device, the C_3H_6 concentration can be estimated from the current under a 1 V application without any interference by oxygen.

Cross sensitivity of the present sensor was further studied, and the responses to NO, NO_2, CO, and H_2 are shown in Figure 10. The current of this sensor was hardly dependent on the concentration of these gases, which are considered as the major coexisting gases in the exhaust gas environment. In our previous study,[14] it was demonstrated that the sensor current, using Pt as the active electrode, monotonically increases with increasing concentration of C_2H_4, C_2H_6, and C_3H_8; however, almost no dependence was observed in the cases of CO_2, H_2O, and CH_4. Hence, considering the cross sensitivity of the sensor using a Pt base active electrode, it can be said that the sensor can selectively detect hydrocarbon except CH_4. Thus, this sensor is ideal for monitoring the unburnt hydrocarbon in the exhaust gas.

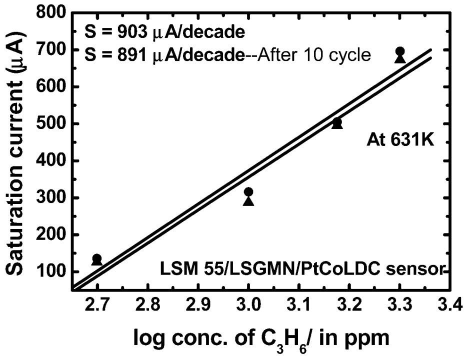

Figure 11. Saturation current change with respect to the C_3H_6 concentration on the sensor as prepared and that after a 10-cycle exposure to 1000 ppm C_3H_6 gas.

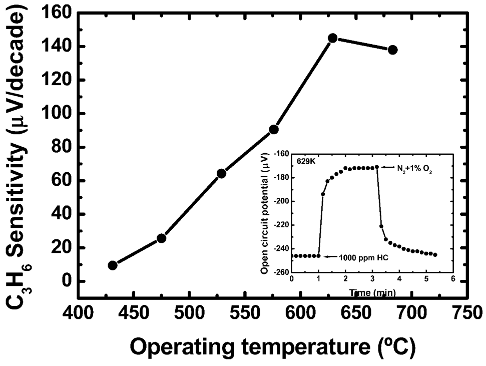

Figure 12. Temperature dependence of the open circuit potential to sense C_3H_6 and the typical sensor response curve (inset) for the LSM 55/LSGMN/Pt–Co–LDC sensor at 623 K.

The stability of the sensor to the harsh environment is also another crucial factor. It is possible that the exhaust gas may sometimes contain very little or no oxygen while the unburnt hydrocarbon is released. This should not degrade the sensor for hydrocarbon combustion in the subsequent time with the availability of sufficient oxygen. To check the stability, the sensor was further investigated. The sensor underwent a cyclic environmental change between 1% O_2 + N_2 and He + 1000 ppm C_3H_6, each with a 5 min duration. Figure 11 shows the saturation current variation of the sensor with respect to the C_3H_6 concentration, before and after such a 10-cycle environmental change. The performance of the sensor after a durability test was found to be almost the same as before with no appreciable change of sensitivity. The base current also remained almost the same. Thus, it could be concluded that the electrode/electrolyte interfaces of the present sensor are very stable for reproducible operation in the exhaust gas environment.

Analysis of Electrode Reactions. To confirm the sensing mechanism, the sensor was also investigated for potentiometric response. The response curve for the open circuit potential is presented in the inset of Figure 12. Although the response was small, a change in the open circuit potential was also observed upon exposure to 1000 ppm C_3H_6. The potential reached the saturation value very fast (within 1 min) and also recovered to the

---

(14) Ishihara, T.; Fukuyama, M.; Dutta, A.; Kabemura, K.; Nishiguchi, H.; Takita, Y. *J. Electrochem. Soc.* **2003**, *150*, H241.

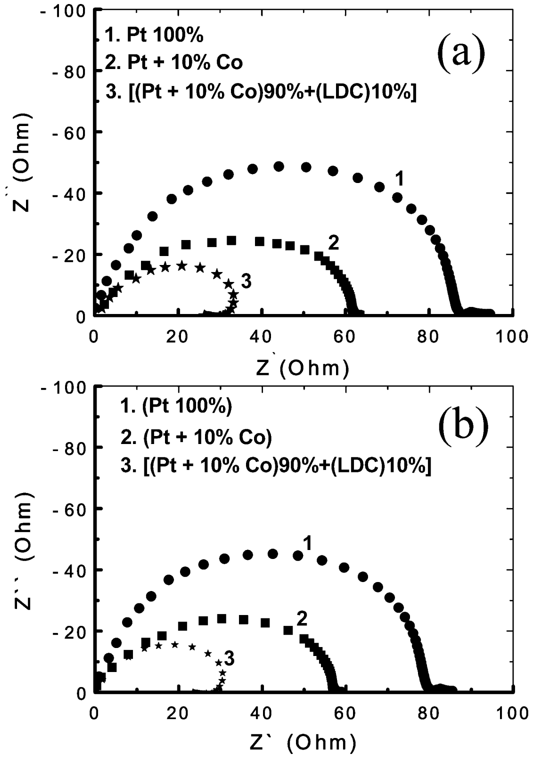

Figure 13. Complex impedance plot for different active electrodes under (a) 1% O_2 in N_2 and (b) 1000 ppm C_3H_6 mixed with 1% O_2 in N_2, at an operating temperature of 623 K in air.

original level within 20−30 s after a change to the base gas N_2 + 1% O_2. Since both electrodes are exposed to the same gaseous environment, the mixed potential appears at each electrode when both oxygen reduction and hydrocarbon oxidation reactions take place on the same electrode. Therefore, the change in current of the present sensor may be related to a change in the mixed potential.[15,16] The applied potential changed with the generation of a mixed potential, and this seems to lead to a change in the oxygen pumping current. The temperature dependency of the sensitivity of such a potentiometric study was found similar in nature to that of the amperometric sensitivity (Figure 12). However, compared with the simple mixed potential, by using an oxygen pumping current, a much larger sensitivity was achieved because of the enhancement of the catalytic activity of the electrodes.

To understand the behavior of the active electrode/solid electrolyte interface, the electrochemical sensor was further studied by impedance spectroscopy analysis at different operating temperatures. Figure 13a shows the complex impedance plot of the sensors with 100% Pt, Pt + 10% Co, and (90% Pt + 10% Co) (90%) + LDC (10%) active electrodes at the best operating temperature of 623 K in the base gas environment under open circuit conditions. All the spectra show one broad semicircle, which corresponds to the electrode overpotential. It is evident that the addition of Co to Pt and subsequent addition of LDC to the Pt−Co system caused a progressive decrease of the resistance sectioned by the semicircle. We can reasonably state that the total impedance decreased at the interface and the decrement is highest for the Pt−Co−LDC system. The observed semicircle in the impedance plot for the Pt-based electrode is not expressed by a simple single semicircle but consists of at least two semicircles on all three electrodes. Therefore, the electrode reaction in the present sensor consists of several intermediate reaction steps, which might be surface adsorption, diffusion, and further electrochemical reaction at the three-phase boundary of the electrode, electrolyte, and gas phase. Comparing the impedance plots, it is seen that the radii of the observed semicircle decreased; namely, addition of Co seems to be effective for decreasing the overpotential of the active electrode of Pt by increasing the surface activity for oxidation. In contrast to Co addition, mixing LDC mainly decreased the impedance at the lower frequency region. In the field of solid oxide fuel cells, it is well-known that mixing an oxide ion conductor with a Ni anode is effective for expanding the reaction area and increasing the electrode activity. In a manner similar to that of the Ni−oxide ion conductor anode, mixing LDC with Pt−Co might expand the effective reaction area for oxidation of hydrocarbon. This is also supported by decreased impedance semicircles appearing at the low-frequency region, because impedance at the low-frequency region is generally assigned to adsorption and diffusion steps.

It was also observed that, in the presence of C_3H_6, the impedance plots follow the same trend as that in base gas, and for individual cases, the resistance intercepted by the impedance semicircle becomes smaller in a sensing gas than that in the base gas, as shown in Figure 13b. Since the pumping current increased upon exposure to sensing gas, the decreased electrode resistance is in good agreement with the observed sensing performance. It is seen that, under a sensing gas condition, the semicircle appearing at the low-frequency region was decreased; however, that at high frequency hardly changed. Assignment of the impedance semicircle is generally difficult, and a further detailed study is required. However, in general, it is known that electrode reaction related to adsorption and diffusion phenomena gives an impedance resistance at the low-frequency region. On a Pt-based electrode, mainly oxidation of C_3H_6 with pumped oxygen ion occurs, resulting in the increased P_{O_2} on the Pt electrode. Therefore, adsorption and diffusion of oxygen might be improved upon exposure to C_3H_6. Doping Co and mixing LDC with Pt improved such surface reaction at the electrode. Thus, impedance resistance at the low-frequency region becomes smaller, and the sensitivity to hydrocarbon is improved.

The temperature dependence of the sensor element on the current output can provide the activation energy (E_a) of the bulk conductivity of the electrolyte. When the electrolyte has a fixed thickness (0.4 mm in this case), the same composition, and the same inactive electrode, we can probably correlate the magnitude of the activation energy with the influence of the active electrode material composition. This means that the lower the activation energy the better the electrode/electrode interface and electrochemical activity therein. Considering this idea in the present work, the temper-

---

(15) Fleming, W. *J. Electrochem. Soc.* **1977**, *124*, 21.
(16) Miura, N.; Raisen, T.; Lu, G.; Yamazoe, N. *Sens. Actuators, B: Chem.* **1998**, *47*, 84.

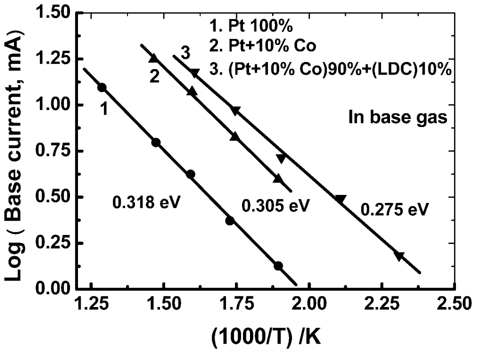

Figure 14. Arrhenius plots of the total electrical conductivity of the sensors with three different active electrode materials under a base gas (1% O_2 in N_2) atmosphere.

ature-dependent activation energy was calculated for different cases from the slope of the log(base current) vs 1/*T* plot under 1 V bias. As shown in Figure 14, the estimated apparent activation energy for the base current changed with metal and cermet addition to Pt. The value of E_a is lowest for the Pt−Co−LDC system, while it is highest for the 100% Pt electrode. This suggests that the surface activity for electrochemical oxidation of hydrocarbon was improved by adding Co and LDC. As a result, the improved sensitivity could be assigned to the increased activity of the anode for oxidation of hydrocarbon. The activation energy was also calculated for a sample in a gas environment. But no significant difference in activation energy value was observed. Although the estimated activation energy does not simply correspond to that of the Pt-based electrode but to the overall reaction on the sensor, a decreased activation energy by doping Co and mixing LDC suggests that the oxidation step on the Pt-based electrode seems to occupy a large part of the apparent activation energy for the pumping current. This might be the reason for the high base current and improved sensitivity to hydrocarbon.

Conclusions

The present study was performed to improve the activity of an LSGMN-based amperometric sensor for C_3H_6 sensing at the low-temperature range (423−673 K) for cold start of an engine. It was found that addition of transition metals enhances the sensitivity. In particular, Co was found the most effective one for increasing the sensitivity to C_3H_6. The most effective amount of Co was 10 wt % against Pt. Mixing an ionic conductor further enhanced the sensitivity and improved the base current of the sensor. Lanthanum-doped ceria was the best material for improvement. And 10% LDC mixed with Pt + 10% Co gave the highest sensitivity. The detection mechanism for the present sensor is now under investigation; however, at present it seems most likely that the mixed potential may contribute to the change in the current. A limiting current type sensor is proposed as the amperometric oxygen and humidity sensor.[17] However, the present sensor is not a limiting current type. This is because the current increases with an increase in applied potential. Since the emf was also changed on exposure to sensing gas (Figure 12), the applied potential could be modified by this emf, resulting in the change of current. The developed amperometric sensor exhibited high sensitivity, stability, and selectivity. As a result, it is highly promising for monitoring uncombusted hydrocarbon in exhaust gas from internal combustion engines. In particular, the highest sensitivity was achieved at a temperature as low as 623 K, and the lowest temperature of detection was 423 K. Hence, for the cold start condition this sensor could be quite useful as the hydrocarbon sensor.

Acknowledgment. We acknowledge financial support from a Grant-in-Aid for Science Promotion (No. 11102006) from the Ministry of Education, Culture, Sports, Science, and Technology.

CM049242E

---

(17) Menil, F.; Coillard, V.; Lucat, C. *Sens. Actuators, B: Chem.* **2000**, *67*, 1.